

Facile Synthesis of Ambient Stable Pyreno[4,5-*b*]pyrrole Monoanion and Pyreno[4,5-*b* : 9,10-*b'*]dipyrrole Dianion: From Serendipity to Design

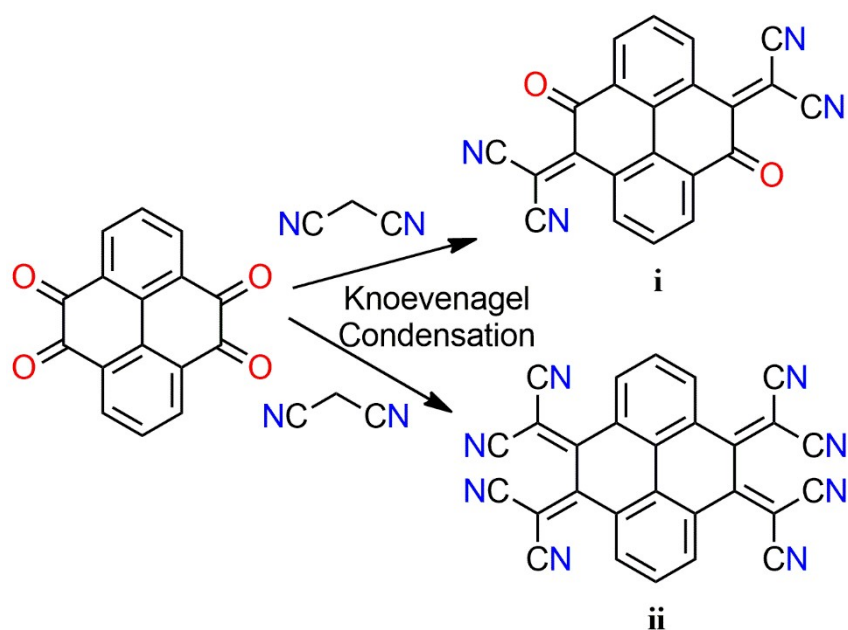
Sharvan Kumar*, Yusuke Hattori, Kohshi Yoshida, Tomohiro Higashino, Hiroshi Imahori, Shu Seki*.

^aDepartment of Molecular Engineering, Graduate School of Engineering, Kyoto University, Nishikyo-ku, Kyoto 615-8510, Japan

Table of Contents

1. Theoretical Details.....	S2
2. Synthetic scheme of proposed molecules.....	S3
3. Synthesis.....	S3
4. Proposed reaction mechanism.....	S6
5. Crystal structures of 1-3 with counter cations.....	S7
6. Optimized structures of 1-3	S7
7. Selected bond lengths of crystal 1-3 and their comparison with optimized structure	S8
8. Crystal structures of 1-3 showing π - π stacking interactions.....	S9
9. Crystal structures of 1-3 showing H-bonding with countercation	S10
10. DPV of compounds 1-3	S11
11. CV of compound 1-3 showing oxidation behaviour.....	S11
12. Photoluminescence spectra of compounds 1-3	S12
13. Table of crystallographic data of 1-3	S13
14. EPR spectra of 1-3	S14
15. FT-IR-Spectra of 1-3	S15
16. ESI-HRMS of 1-3	S16
17. NMR.....	S19
18. References.....	S23

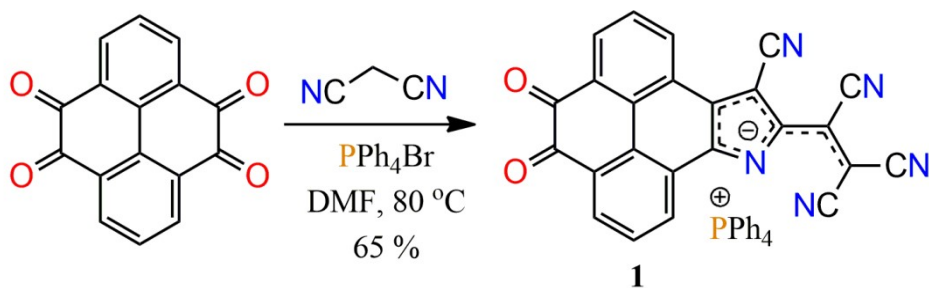
Theoretical Details: The ground-state geometry optimization of the investigated structures was carried out in gas phase at the Becke three-parameter¹ hybrid exchange functional in concurrence with the Lee-Yang-Parr gradient-corrected correlation function (B3LYP functional)² level of the density functional theory (DFT), using the 6-311++G(d,p) basis set. DFT calculations have been performed on all stationary points of the potential energy surface (PES) and studied using the Gaussian 16, Revision C.01.³ The geometries were optimized without any constrain. Counter cations were not used in calculation. The HOMO-LUMO analysis was performed using DFT optimized structures with IEFPCM model in CH₂Cl₂ and plotted with the Gauss View 6.0.9 program.



Scheme S1: Proposed molecules (**i** and **ii**) and designed synthetic route.

Synthesis of Pyrene-4,5-dione and Pyrene-4,5,9,10-tetraone: The starting compound pyrene-4,5-dione and Pyrene-4,5,9,10-tetraone were synthesized using reported procedure.⁴

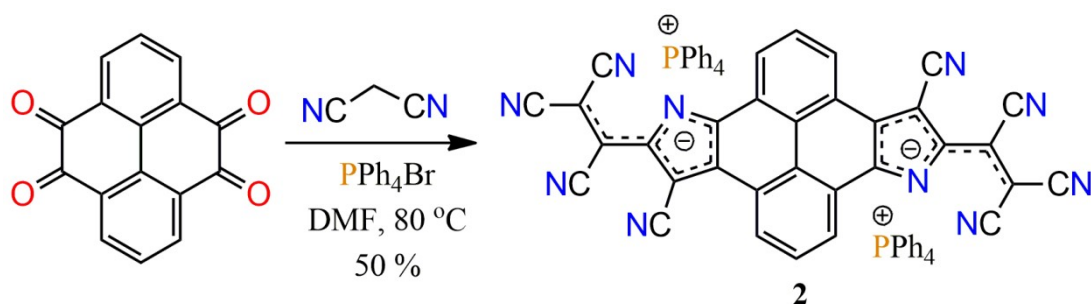
Synthesis of pyreno[4,5-dioxo-9,10-b]pyrrole monoanion (1**):**



In a 50 mL round bottom flask containing (100 mg, 0.38 mmol) pyrene-4,5,9,10-tetraone and (480 mg, 1.14 mmol) tetraphenylphosphonium bromide (PPh₄Br), 4.0 mL anhydrous DMF was added and the mixture was heated at 80°C for 10 minutes with stirring. Thereafter, (75 mg, 1.14 mmol) malononitrile was added in to it and the mixture was heated at same temperature for next 30 minute. The reaction mixture was cooled to room temperature and precipitated using excess diethyl ether and a few mL of hexane. The precipitate was collected by centrifuging and dried. The dried precipitate was purified by silica gel column chromatography using THF: Hexane (2.0: 1.3) Yield = 65 %. R_f = 0.55 (9: 1 THF/Hexane). M. P.: 295 °C. ¹H NMR (400 MHz, CD₂Cl₂, 298 K, TMS): δ (ppm) = 9.04 (d, *J* = 8.4 Hz, 1H), 8.89 (d, *J* = 8.4 Hz, 1H), 8.25 (t, *J* = 8.4 Hz, 2H), 3.32 (m, 6H), 7.91-7.53 (m, 22H). ¹³C

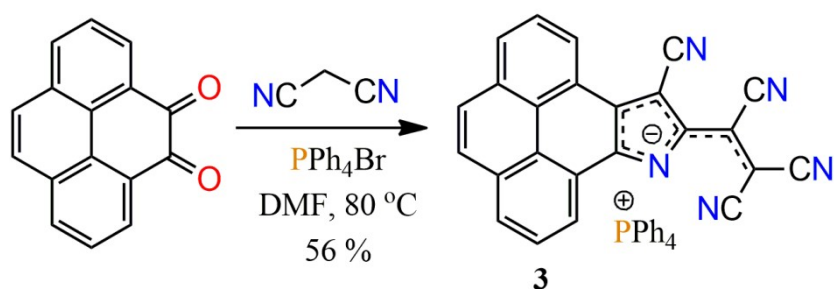
NMR (100 MHz, CD₂Cl₂, 298 K, TMS): δ (ppm) = 181.25, 136.27, 134.93, 134.83, 132.00, 131.39, 131.34, 131.15, 131.02, 130.89, 129.54, 129.99, 128.90, 128.77, 128.60, 118.43, 117.53, 114.34, 97.04. ESI-HRMS: calculated for [C₂₄H₆N₅O₂⁻ (anion)] (m/z) 396.0527, found 396.0524, and for [C₂₄H₂₀P⁺ (cation)] m/z 339.1297, found 339.1304. FT-IR (neat, cm⁻¹): 3078, 3058, 3023, 2993, 2971, 2208, 1746, 1667, 1597, 1553, 1520, 1495, 1452, 1437, 1415, 1398, 1365, 1340, 1315, 1285, 1246, 1172, 1152, 1107, 1046, 1028, 997, 919, 802, 756, 722, 712, 687, 643, 595, 525.

Synthesis of pyreno[4,5-b, 9,10-b]dipyrrole dianion (2):



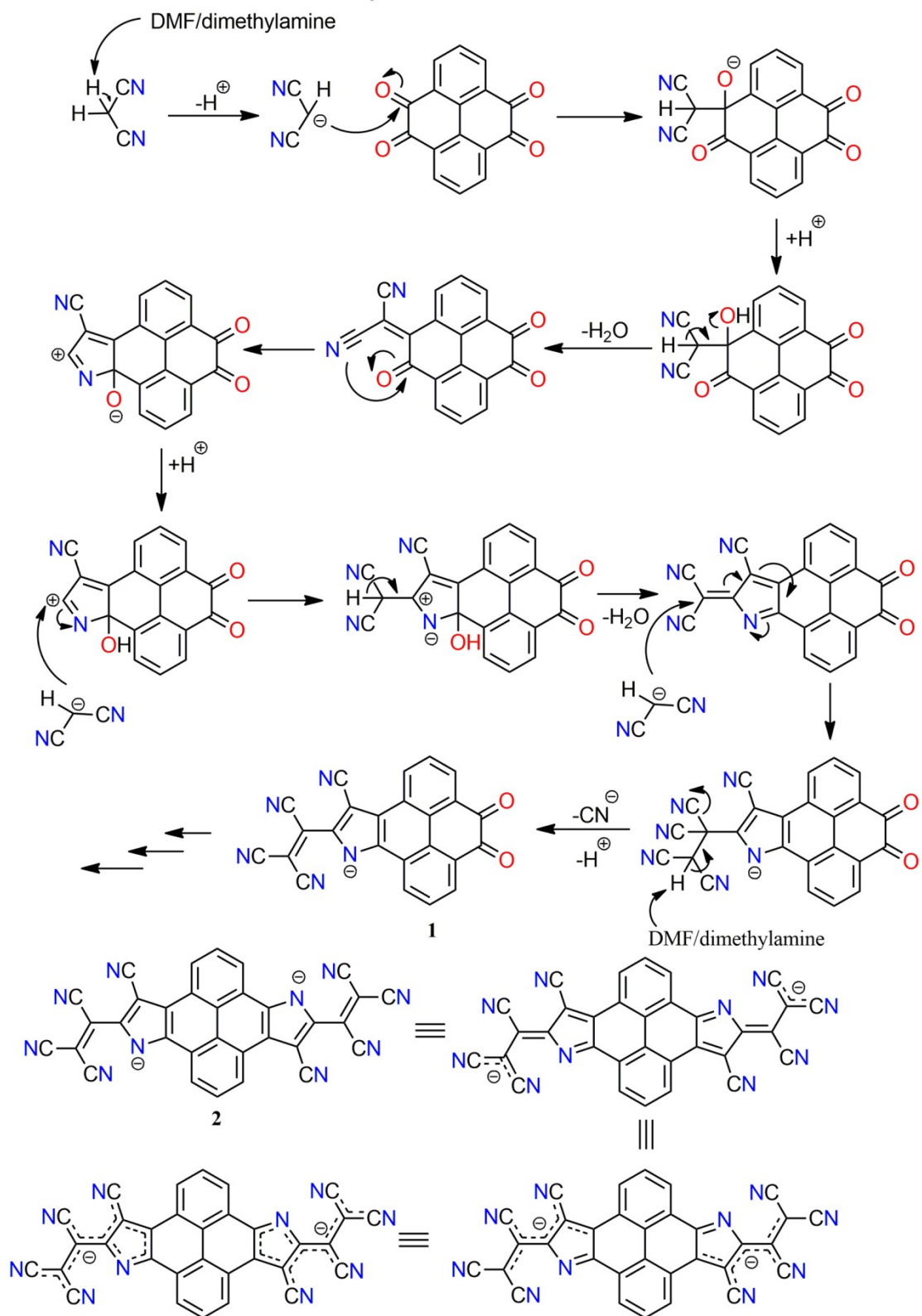
In a 50 mL round bottom flask containing (100 mg, 0.38 mmol) pyrene-4,5,9,10-tetraone and (800 mg, 1.91 mmol) tetraphenylphosphonium bromide (PPh₄Br), 4.0 mL anhydrous DMF was added and the mixture was heated at 80 °C for 10 minutes with stirring. Thereafter, (151 mg, 2.28 mmol) malononitrile was added in to it and the mixture was heated at same temperature for next 30 minute. The reaction mixture was cooled to room temperature and precipitated using excess diethyl ether and a few mL of hexane. The precipitate was collected by centrifuging and dried. The dried precipitate was purified by silica gel column chromatography using THF: Hexane (2.0: 1.0) Yield = 50 %. R_f = 0.45 (9: 1 THF/Hexane). M. P.: 244-246 °C. ¹H NMR (400 MHz, CDCl₃, 298 K, TMS): δ (ppm) = 8.72 (m, 2H), 8.51 (m, 2H), 7.73-7.766 (m, 8H) 7.58-7.48 (m, 18H), 7.38-7.28 (m, 16H). ¹³C NMR (100 MHz, CDCl₃, 298 K, TMS): δ (ppm) = 136.08, 136.05, 134.75, 134.65, 130.87, 128.84, 128.42, 127.25, 127.12, 126.92, 124.31, 122.94, 122.78, 122.44, 122.24, 118.85, 118.27, 117.38, 117.01, 116.55, 115.02, 93.89. ESI-HRMS: calculated for [C₃₂H₆N₁₀²⁻ (dianion)] (m/2) 265.0395, found 265.0394, and for [2C₂₄H₂₀P⁺ (cation)] (m/z) 339.1297, found 339.1302. FT-IR (neat, cm⁻¹): 3089, 3064, 3029, 2993, 2969, 2204, 1736, 1588, 1521, 1476, 1438, 1396, 1361, 1330, 1268, 1180, 1154, 1107, 1069, 1047, 997, 983, 935, 798, 755, 720, 687, 523.

Synthesis of pyreno[4,5-b]pyrrole monoanion (3):



In a 50 mL round bottom flask containing (100 mg, 0.43 mmol) pyrene-4,5-dione and (542 mg, 1.29 mmol) tetraphenylphosphonium bromide (PPh₄Br), 4.0 mL anhydrous DMF was added and the mixture was heated at 80 °C for 10 minutes with stirring. Thereafter, (85 mg, 1.29 mmol) malononitrile was added in to it and the mixture was heated at same temperature for next 30 minute. The reaction mixture was cooled to room temperature and precipitated using excess diethyl ether and a few mL of hexane. The precipitate was collected by centrifuging and dried. The dried precipitate was purified by silica gel column chromatography using THF: Hexane (2.0: 1.0) Yield = 56 %. R_f = 0.35 (9: 1 THF/Hexane). M. P.: 110 °C. ¹H NMR (400 MHz, CDCl₃, 298 K, TMS): δ (ppm) = 8.99 (d, J = 7.6 Hz, 1H), 8.75 (d, J = 7.2 Hz, 1H), 8.04-8.01 (m, 2H) 7.94 (b, 2H), 7.89-7.84 (m, 6H), 7.72-7.76 (m, 8H), 7.56-7.51 (m, 8H). ¹³C NMR (100 MHz, CDCl₃, 298 K, TMS): δ (ppm) = 136.18, 134.88, 131.11, 127.90, 127.58, 127.08, 126.69, 126.59, 126.12, 122.04, 122.00, 118.56, 117.49, 116.86, 116.40, 114.86, 94.32. ESI-HRMS: calculated for [C₂₄H₈N₅⁻ (anion)] (m/z) 366.0785, found 366.0783, and for [C₂₄H₂₀P⁺ (cation)] (m/z) 339.1301, found 339.1302. FT-IR (neat, cm⁻¹): 3169, 3144, 3055, 3042, 2195, 1742, 1585, 1530, 1504, 1468, 1434, 1406, 1384, 1330, 1339, 1273, 1230, 1173, 1153, 1107, 1068, 1050, 997, 900, 828, 754, 717, 687, 523.

Proposed Reaction Mechanism



Scheme S2: Proposed plausible reaction mechanism of 1-3.

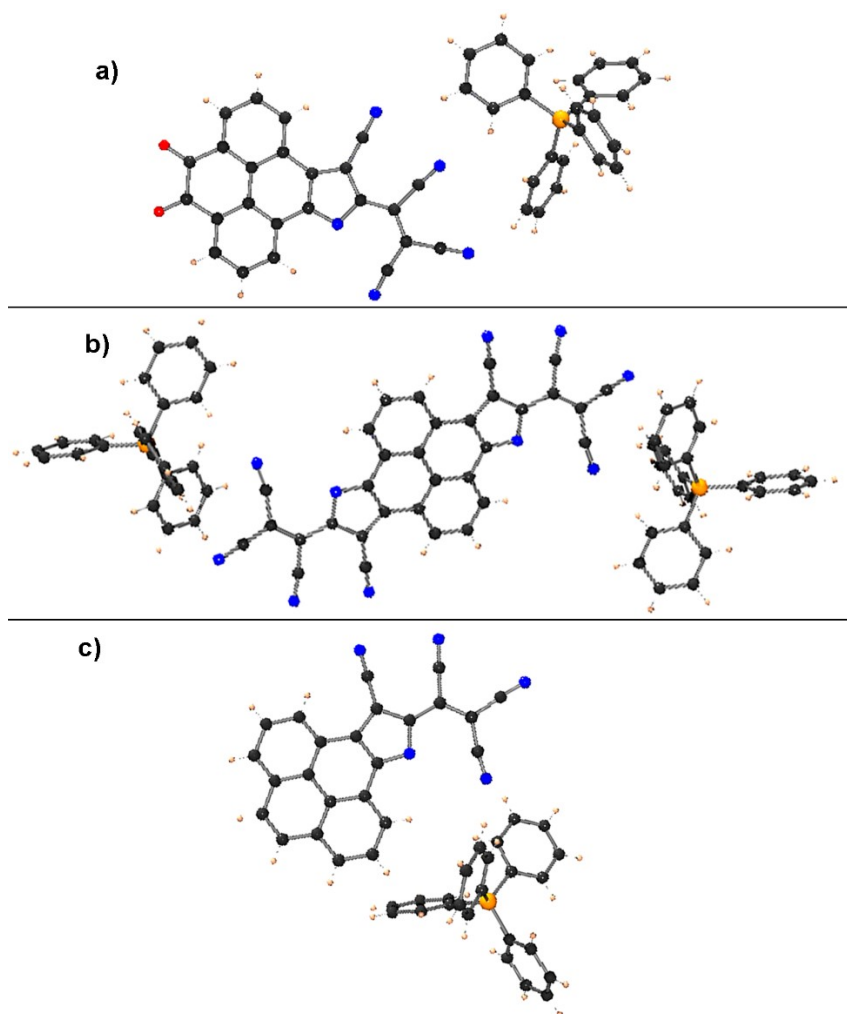


Figure S1: POV-Ray depiction of the crystal structure of a) **1**, b) **2**, and c) **3** with counter cations.

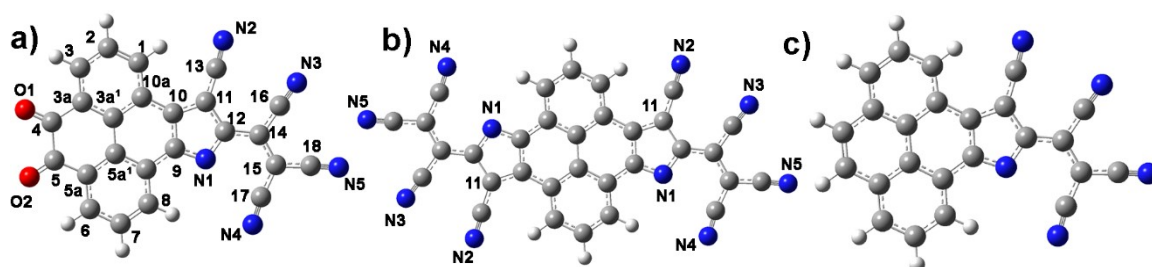


Figure S2: Optimized structures of **1**, **2** and **3** at B3LYP/6-311++G(d,p) DFT level of theory with IEFPCM model in CH_2Cl_2 . The global minimum energy for **1**, **2** and **3** molecules were found to be -1342.82878069, -1771.18304068, and -1193.55414099 Hartrees, respectively. To save the computational time, counter anions were omitted. Numbering is used for denoting the crystallographic and optimized structures bond length (To make it simple we used same numbering for all the anions).

Table S1: A comparison of the selected bond lengths (Å) of X-ray crystal structures of **1**, **2**, and **3** with the geometry optimized structures of **1**, **2**, and **3**.

Bond	Crystal data			Theor. data		
	1	2	3	1	2	3
C1-C2	1.3812	1.3684	1.3672	1.3859	1.3883	1.3957
C2-C3	1.3909	1.3957	1.3842	1.3924	1.3918	1.3854
C3-C3a	1.3711	1.4061	1.3889	1.3943	1.4041	1.4067
C3a-C4	1.4814	1.4574	1.4556	1.4814	1.4465	1.4361
C3a-C3a ¹	1.4145	1.4125	1.4144	1.4184	1.4322	1.4255
C4-C5	1.5184	1.4223	1.4227	1.5530	1.4302	1.3580
C5-C5a	1.4689	1.4617	1.4367	1.4780	1.4433	1.4348
C5a-C6	1.3779	1.3983	1.3985	1.3948	1.4009	1.4071
C5a-C5a ¹	1.4154	1.4313	1.4242	1.4191	1.4225	1.4256
C6-C7	1.3810	1.3684	1.3726	1.3955	1.3553	1.3882
C7-C8	1.3865	1.3957	1.3807	1.3852	1.3818	1.3952
C8-C8a	1.3916	1.4061	1.4072	1.4075	1.4041	1.3970
C8a-C9	1.4370	1.4574	1.4356	1.4386	1.4465	1.4416
C9-C10	1.4140	1.4223	1.3543	1.4242	1.4302	1.4287
C10-C10a	1.4525	1.4617	1.4314	1.4434	1.4439	1.4458
C3a ¹ -C5a ¹	1.4588	1.4712	1.4516	1.4619	1.4595	1.4409
C4-O1	1.2171	-	-	1.2147	-	-
C5-O2	1.2280	-	-	1.2149	-	-
C9-N1	1.3446	1.3457	1.3408	1.3366	1.33518	1.3358
C10-C11	1.3946	1.3692	1.3966	1.4130	1.4088	1.4111
C11-C12	1.4215	1.4403	1.4363	1.4439	1.4514	1.4461
C11-C13	1.4314	1.4199	1.4168	1.4104	1.4100	1.4103
C12-C14	1.4210	1.4671	1.4121	1.4299	1.4202	1.4264
C14-C15	1.3774	1.3764	1.3917	1.3943	1.4050	1.3978
C14-C16	1.4420	1.4011	1.4301	1.4345	1.4352	1.4347
C15-C17	1.4276	1.4615	1.4125	1.4250	1.4227	1.4242
C15-C18	1.4313	1.3851	1.4276	1.4243	1.4216	1.4235
C13-N2	1.1602	1.1812	1.1484	1.1598	1.1650	1.1600
C16-N3	1.1483	1.1929	1.1493	1.1548	1.1553	1.1550
C17-N4	1.1462	1.1469	1.1401	1.1579	1.1592	1.1584
C18-N5	1.1543	1.1787	1.1484	1.1581	1.1600	1.1587
C12-N1	1.3631	1.3675	1.3681	1.3559	1.3594	1.3571

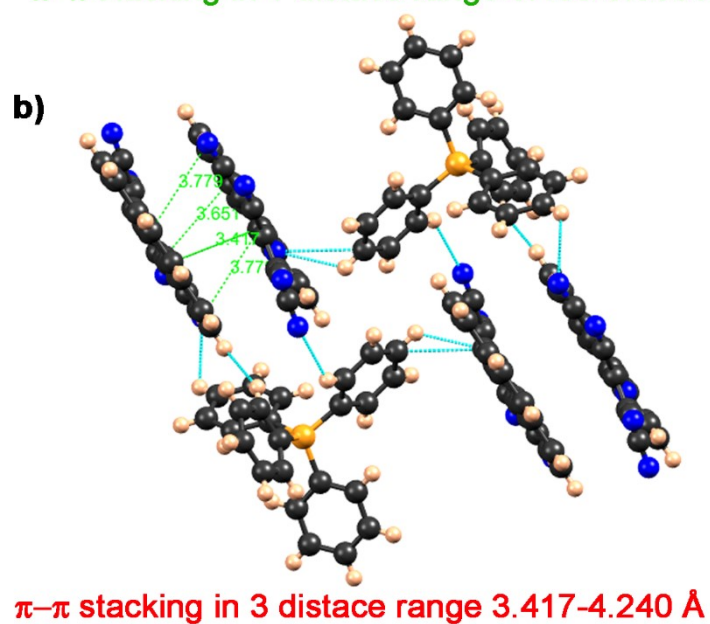
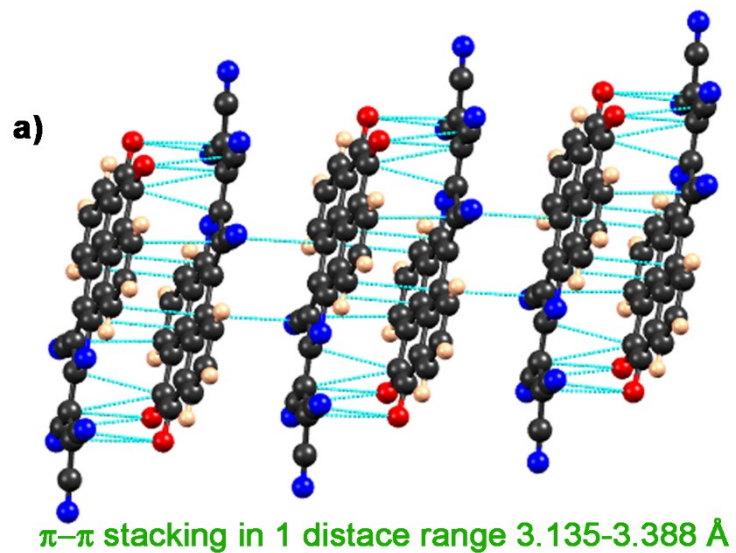


Figure S3: Crystal structure of a) 1 and b) 3 showing the face-to-face π - π interactions.

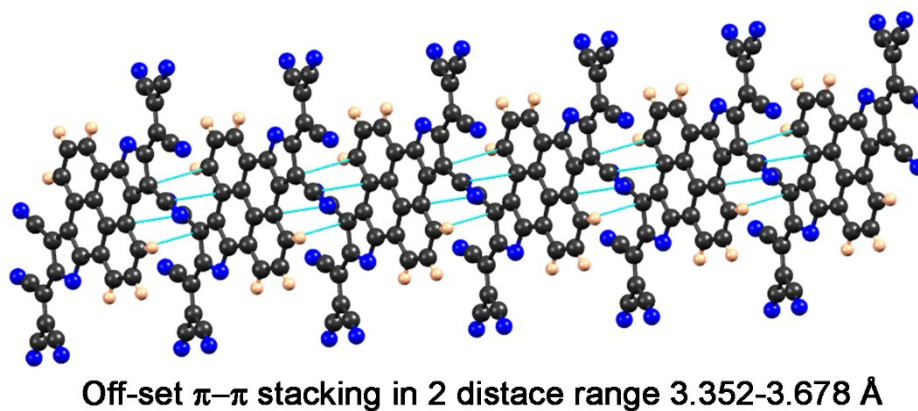


Figure S4: Crystal structure of 2 showing off-set π - π interactions.

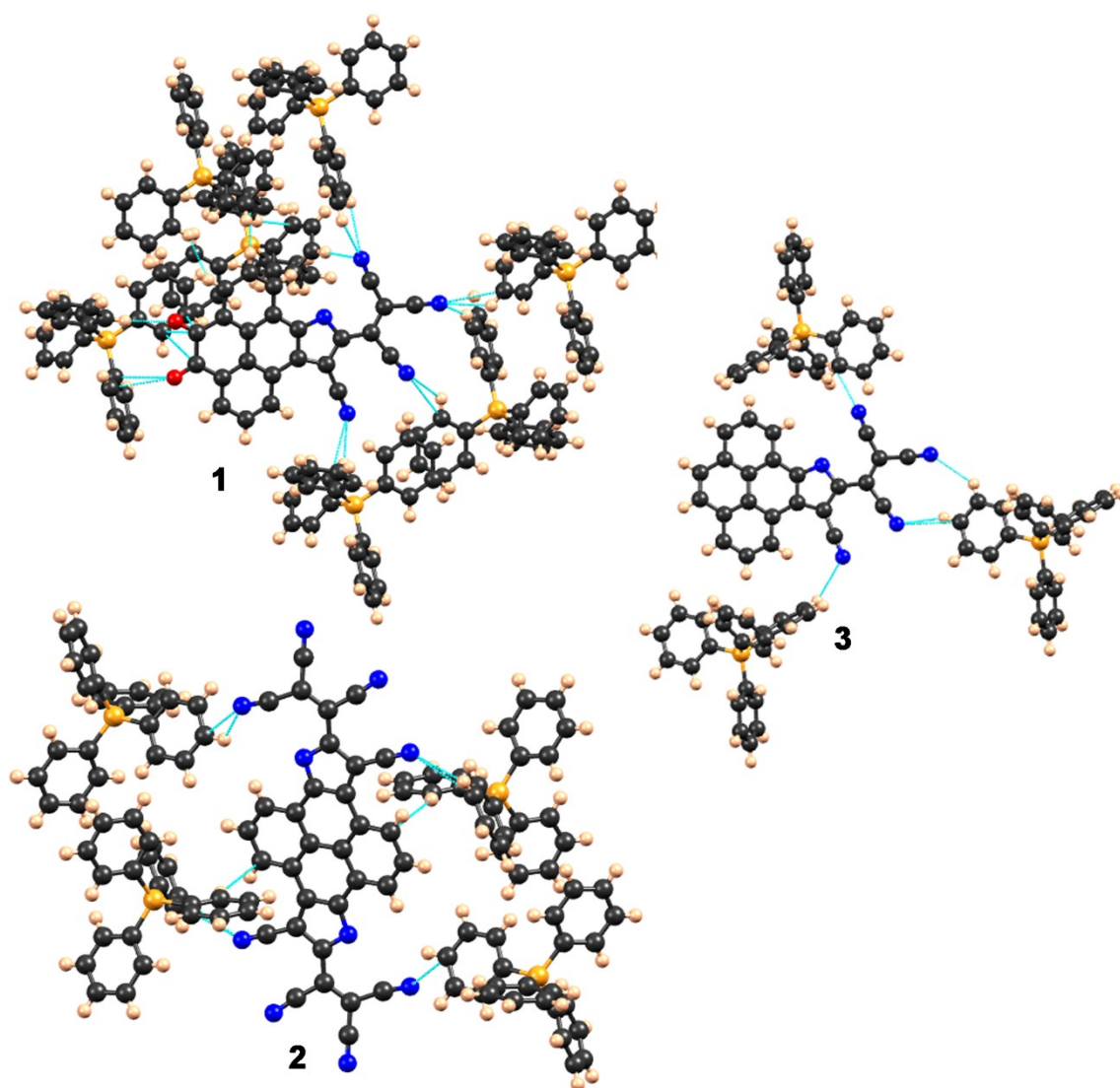


Figure S5: Crystal structure of 1, 2, and 3 showing the H-bonding with counter cation.

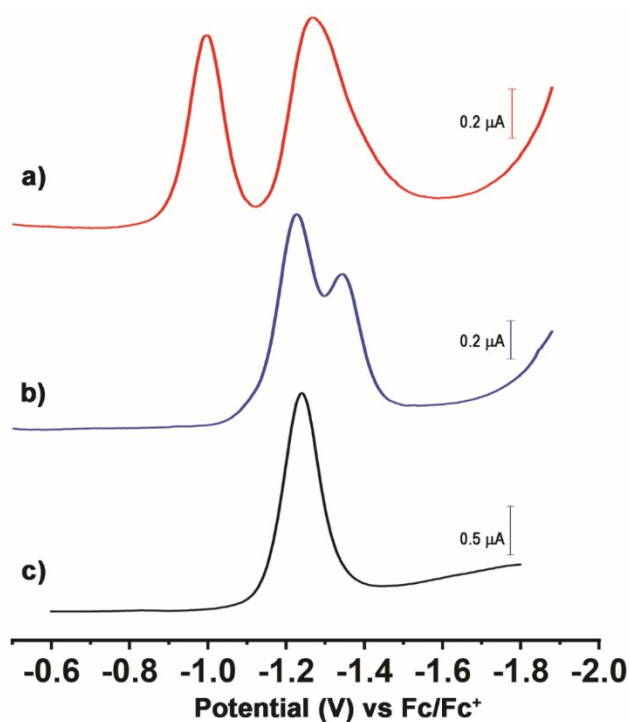


Figure S6: DPV of anions a) **1**, b) **2**, and c) **3**. Conditions: 5×10^{-4} M in DCM; reference electrode, Ag/AgCl; working and auxiliary electrodes, Pt with 0.1 M *n*-Bu₄NBF₄ and (Fc/Fc⁺); 298 K; scan rate, 200 mV/s.

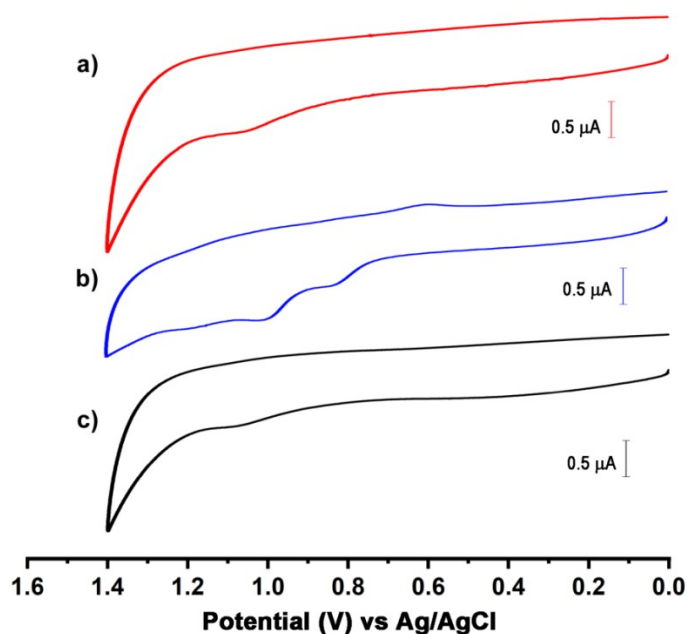


Figure S7: CV of anions a) **1**, b) **2**, and c) **3** showing the oxidation behaviour. Conditions: 5×10^{-4} M in DCM; reference electrode, Ag/AgCl; working and auxiliary electrodes, Pt with 0.1 M *n*-Bu₄NBF₄ and (Ag/AgCl); 298 K; scan rate, 200 mV/s.

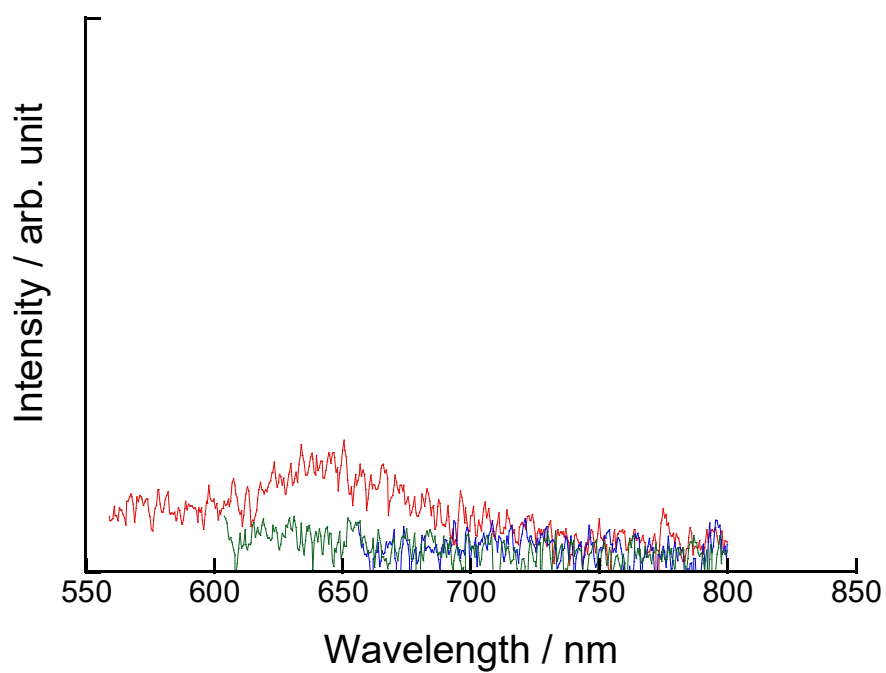


Figure S8: Photoluminescence spectra recorded in CH₂Cl₂ solutions of compounds **1**(red), **2**(blue), and **3**(green) at 1×10^{-5} mol dm⁻³ conc. Excitation was carried out at 550, 650, and 600 nm for **1**, **2**, and **3**, respectively.

Table S2: Crystallographic data for molecule **1**, **2**, and **3**.

	1	2	3
Empirical formula	C ₂₄ H ₆ N ₅ O ₂ , C ₂₄ H ₂₀ P	C ₃₂ H ₆ N ₁₀ , 2(C ₂₄ H ₂₀ P)	C ₂₄ H ₈ N ₅ , C ₂₄ H ₂₀ P
Formula weight	735.71	1209.23	705.72
Temperature/K	153(2)	153(2)	183(2)
Crystal system	triclinic	monoclinic	triclinic
Space group	<i>P</i> -1	<i>P</i> 2 ₁ / <i>n</i>	<i>P</i> -1
a/Å	9.287(4)	7.529(2)	11.934(2)
b/Å	14.079(6)	30.222(9)	13.207(2)
c/Å	14.828(6)	13.985(4)	14.026(3)
α/°	99.420(5)	90	117.428(8)
β/°	100.745(6)	92.770(4)	103.381(10)
γ/°	104.380(5)	90	100.452(16)
Volume/Å ³	1799.6(13)	3178.4(16)	1799.7(6)
Z	2	4	2
ρ _{calc} /cm ³	1.358	1.387	1.302
μ/mm ⁻¹	0.127	0.210	0.120
F(000)	760.0	1336.0	732.0
2θ range for data collection/°	3.013 to 27.498	3.026 to 27.465	3.025 to 26.995
Reflections collected	14684	21495	14025
Independent reflections	7885	7059	7549
Goodness-of-fit on F ²	1.025	1.020	1.031
R1 [I>=2σ(I)]	0.0570	0.0889	0.0595
wR2(reflection)	0.1176	0.2445	0.1458

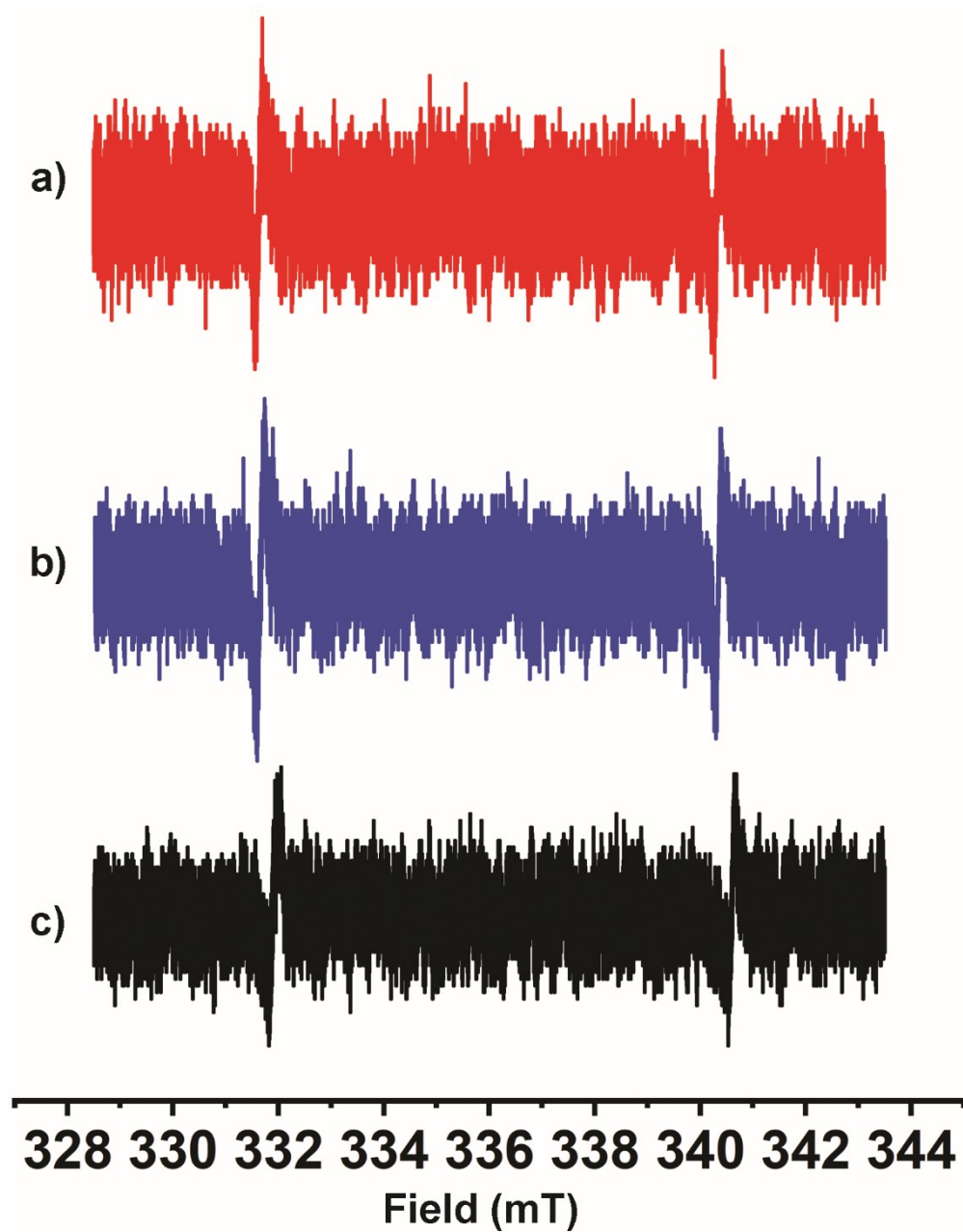


Figure S9: Solution state X-band EPR spectra of a) **1**; b) **2**; and c) **3**. Conditions; 5×10^{-3} M in DCM. No EPR signal was found.

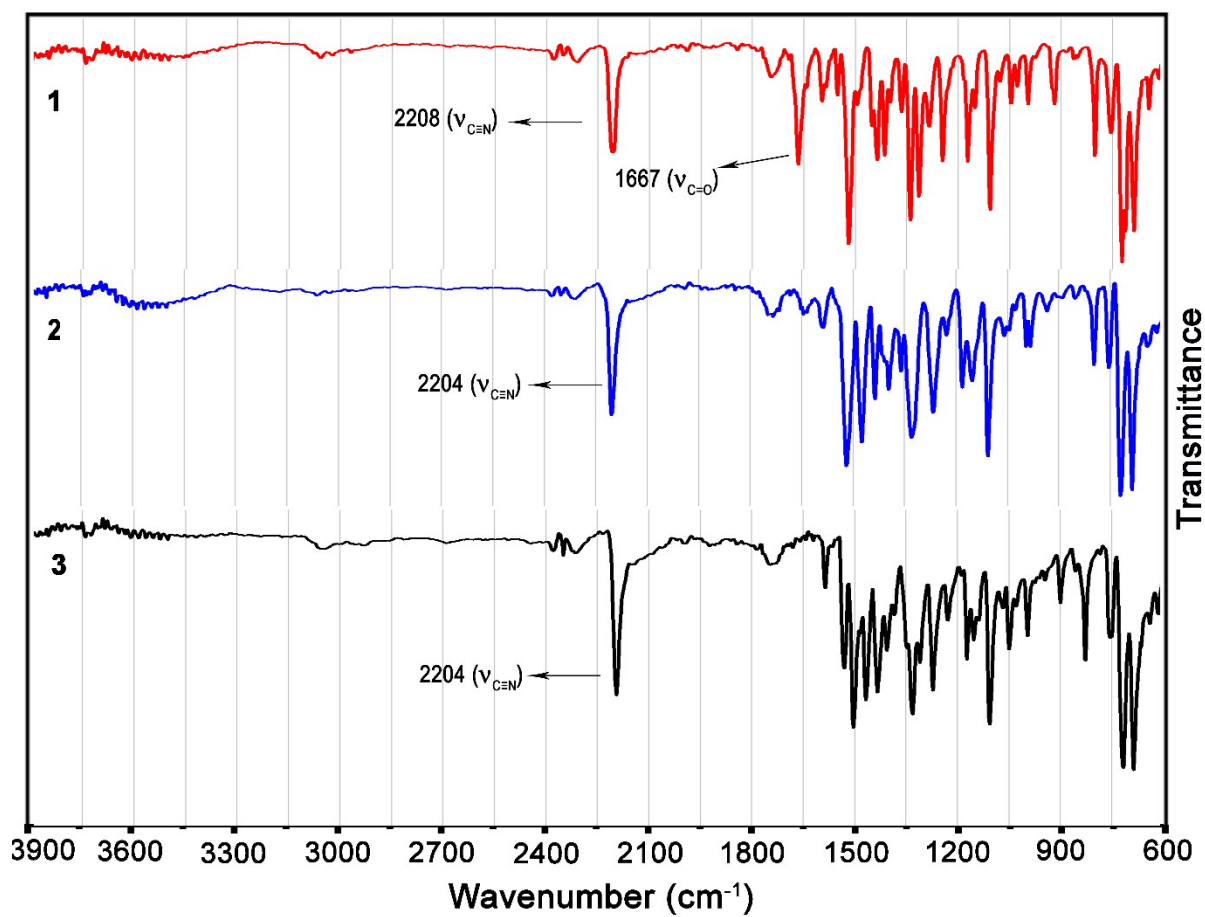


Figure S10: FT-IR spectra of compounds **1**, **2** and **3** neat.

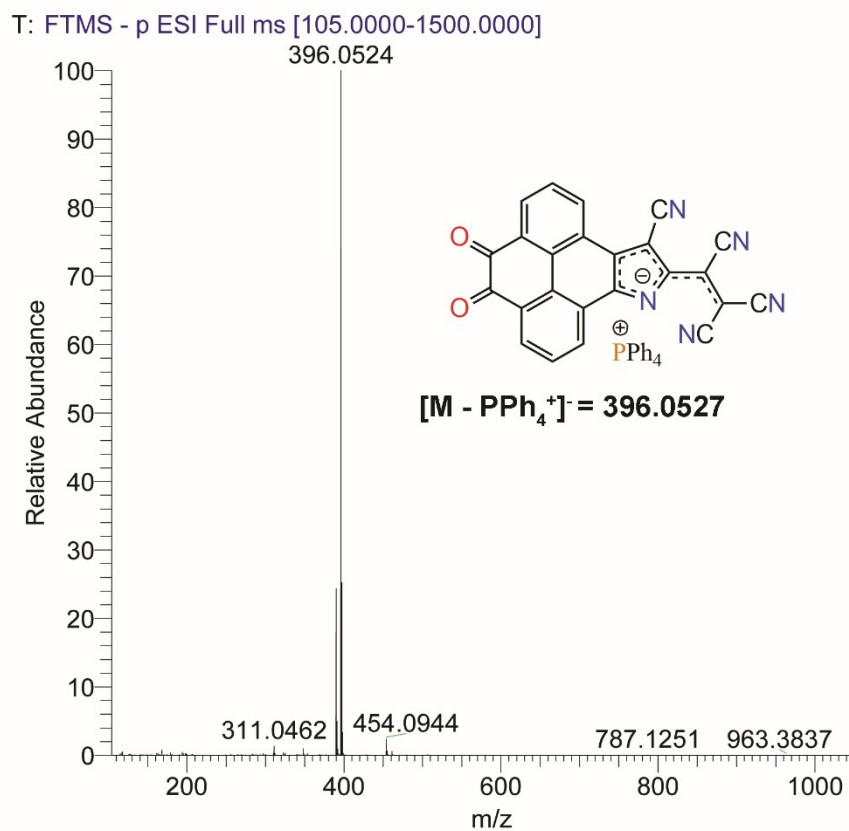


Figure S11: ESI-HRMS of molecule **1** (anion part).

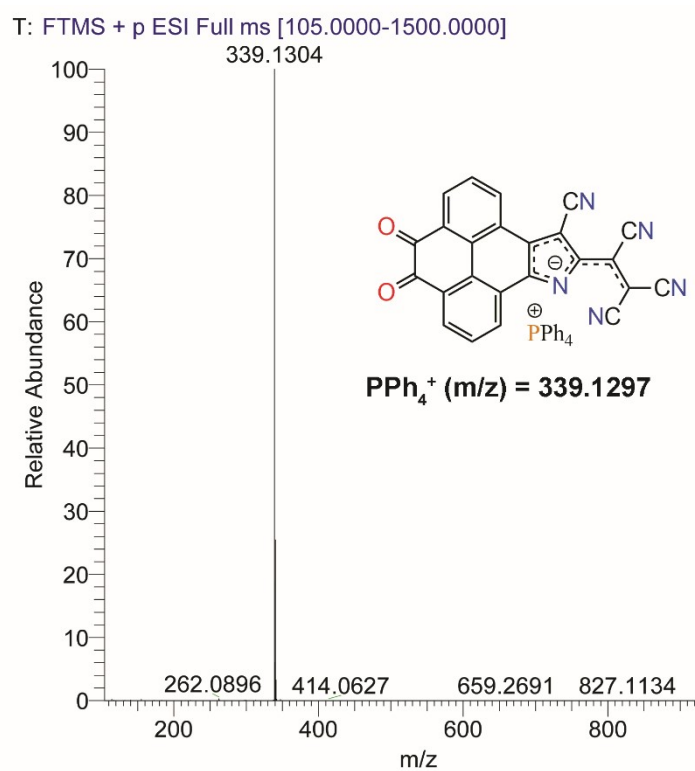


Figure S12: ESI-HRMS of molecule **1** (cation part).

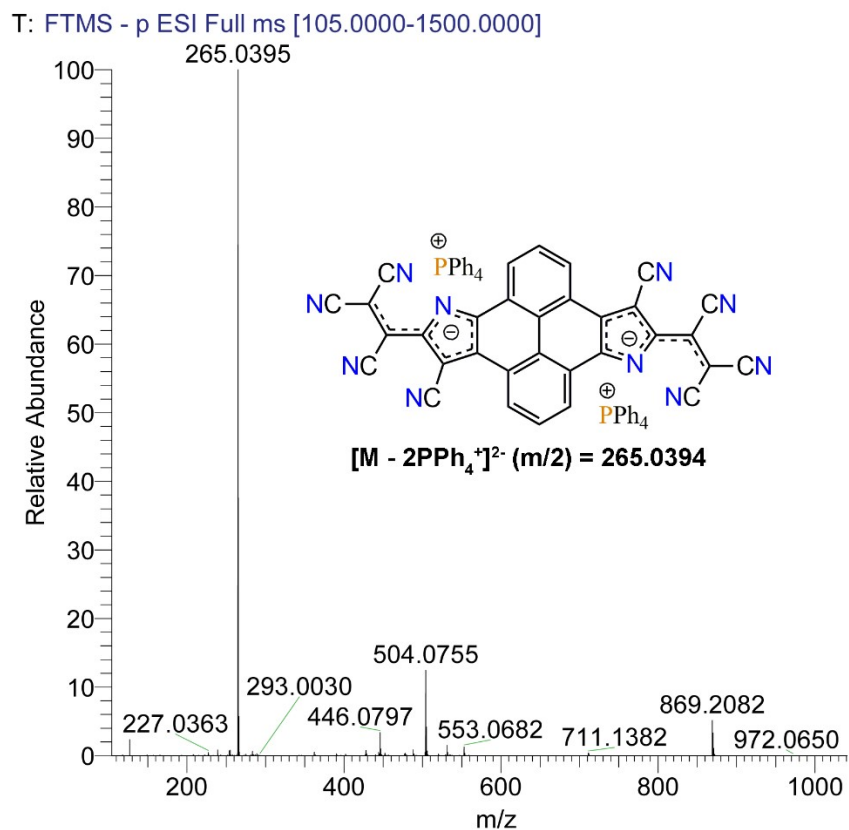


Figure S13: ESI-HRMS of molecule **2** (anion part).

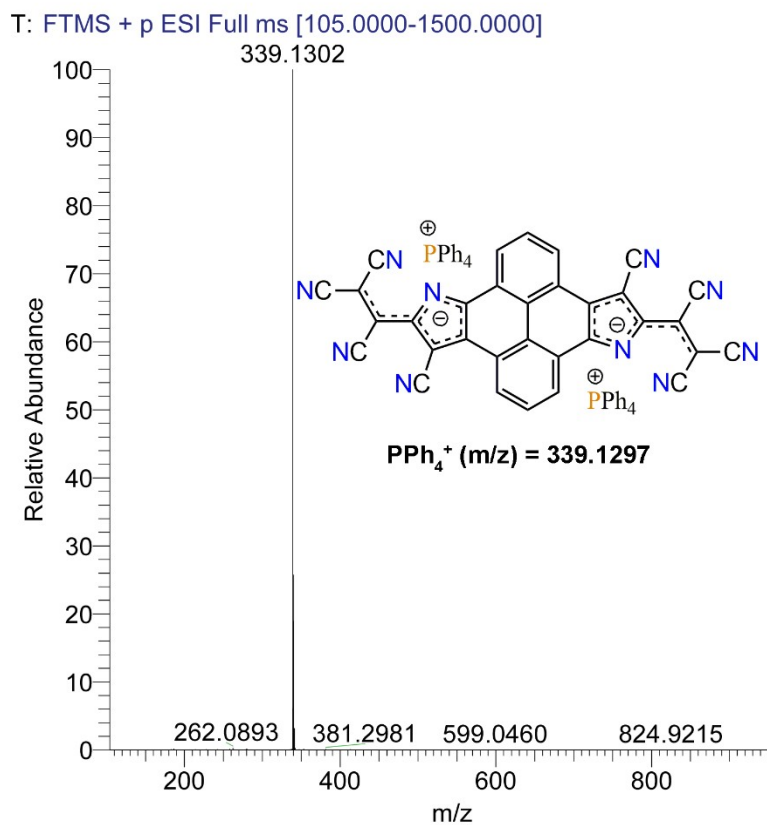


Figure S14: ESI-HRMS of molecule **2** (cation part).

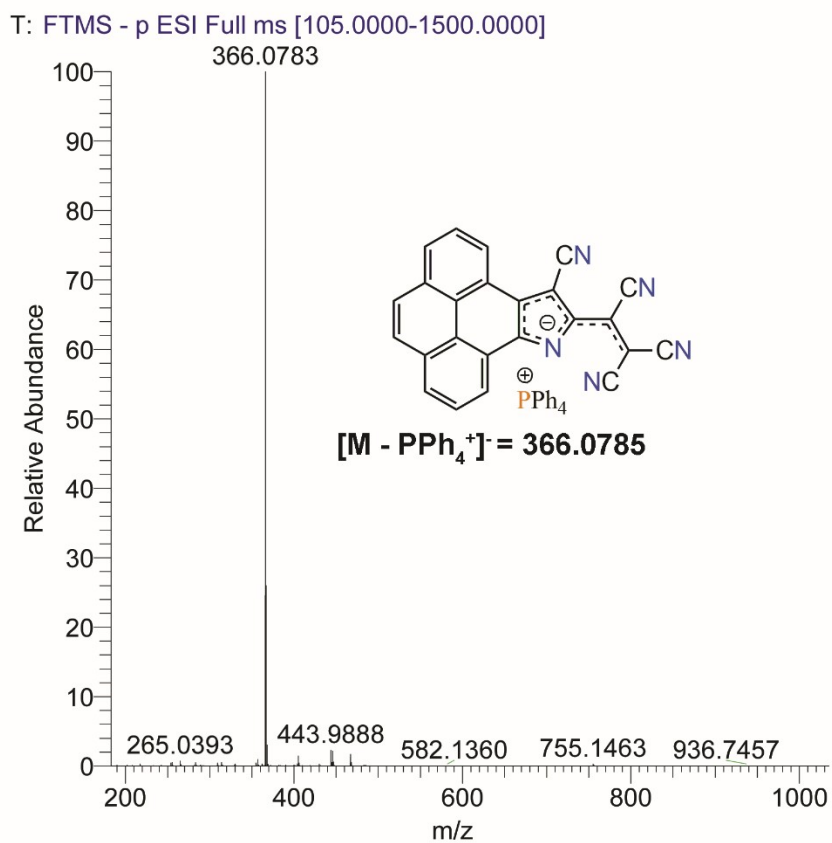


Figure S15: ESI-HRMS of molecule **3** (anion part).

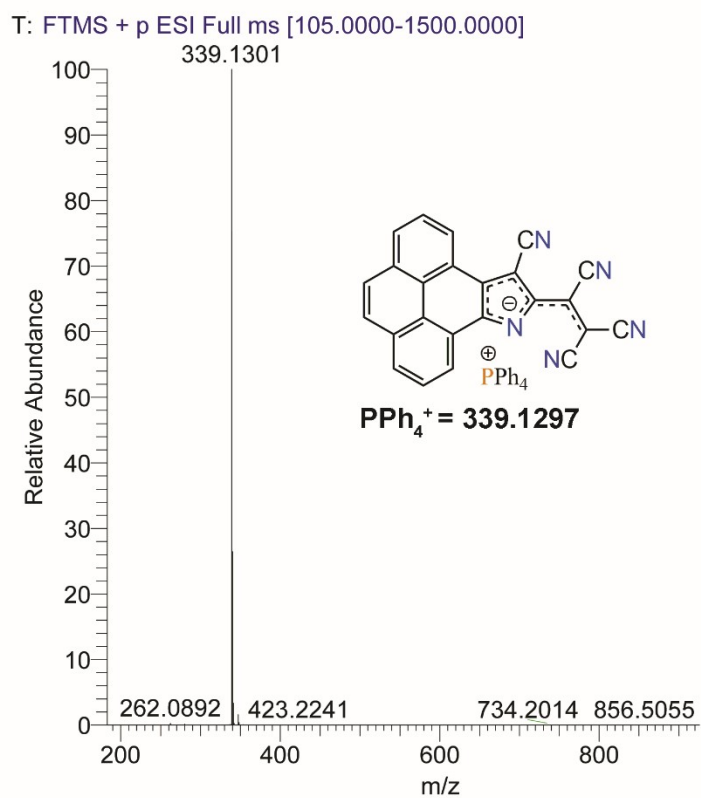


Figure S16: ESI-HRMS of molecule **3** (cation part).

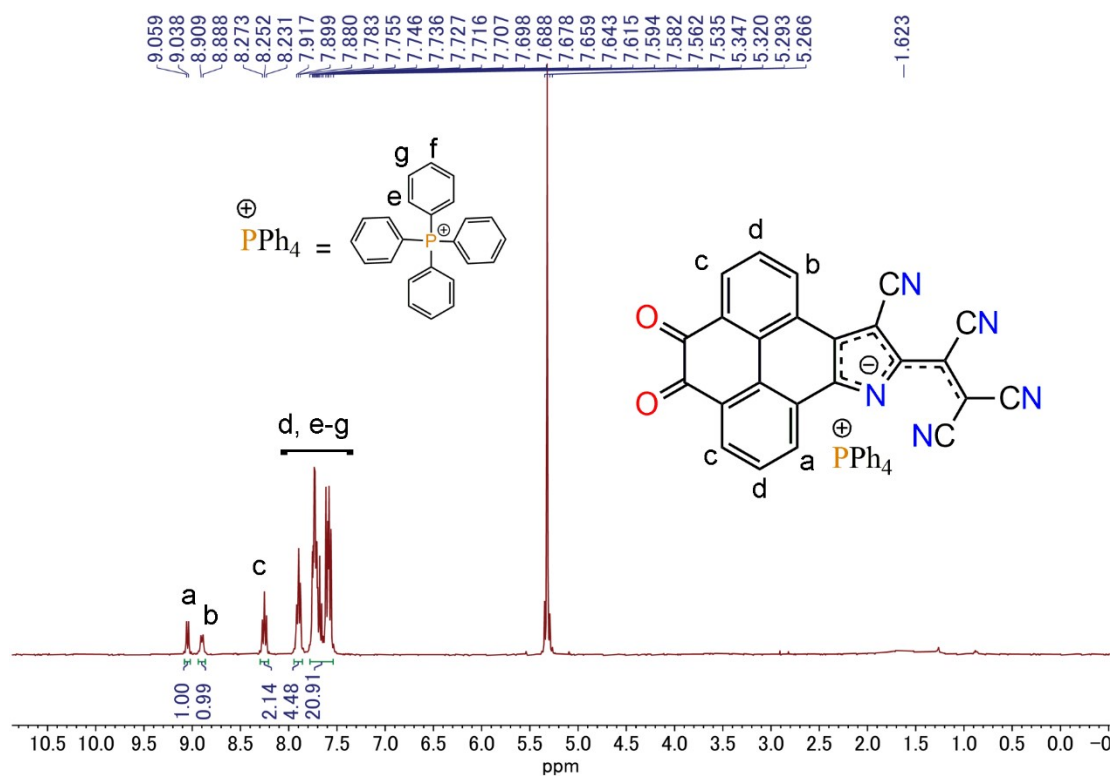


Figure S17: 400 MHz ^1H NMR spectrum of molecule **1** at RT in CD_2Cl_2 .

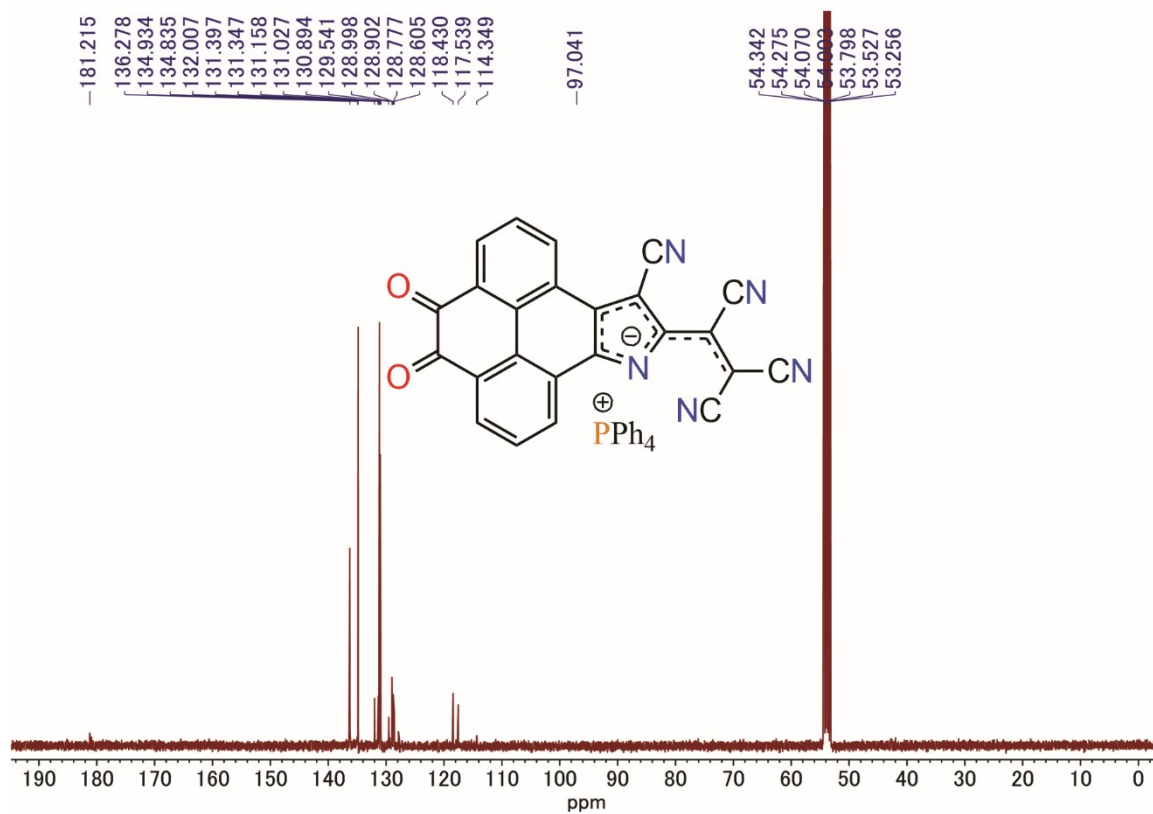


Figure S18: 100 MHz ^{13}C NMR spectra of molecule **1** at RT in CD_2Cl_2 .

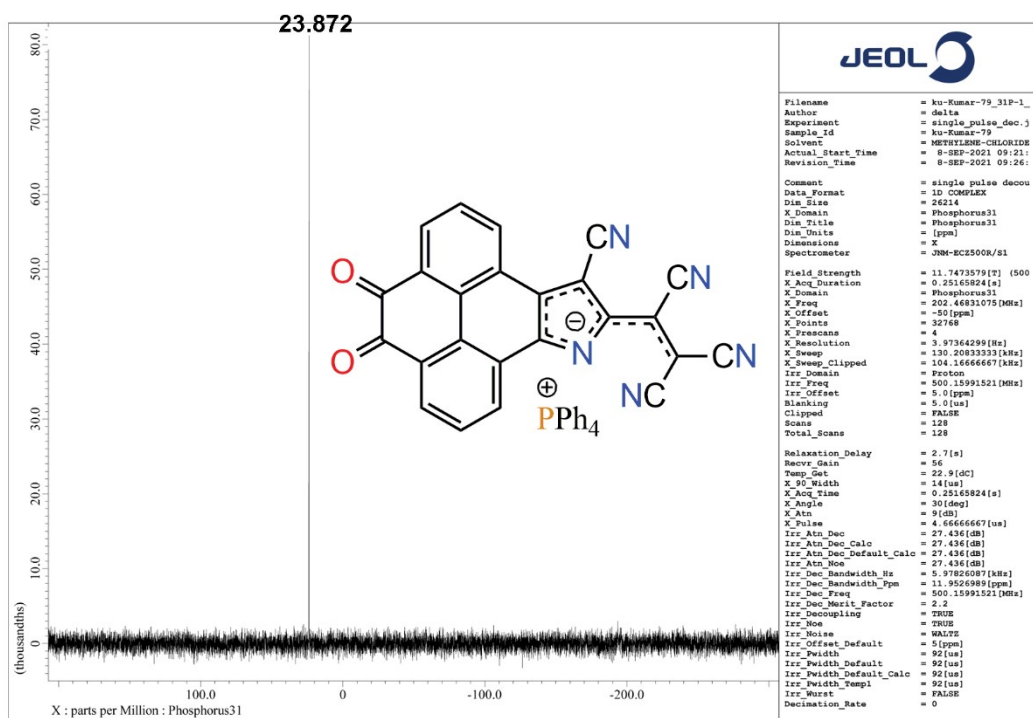


Figure S19: 202 MHz ^{13}P NMR spectrum of molecule **1** at RT in CD_2Cl_2 .

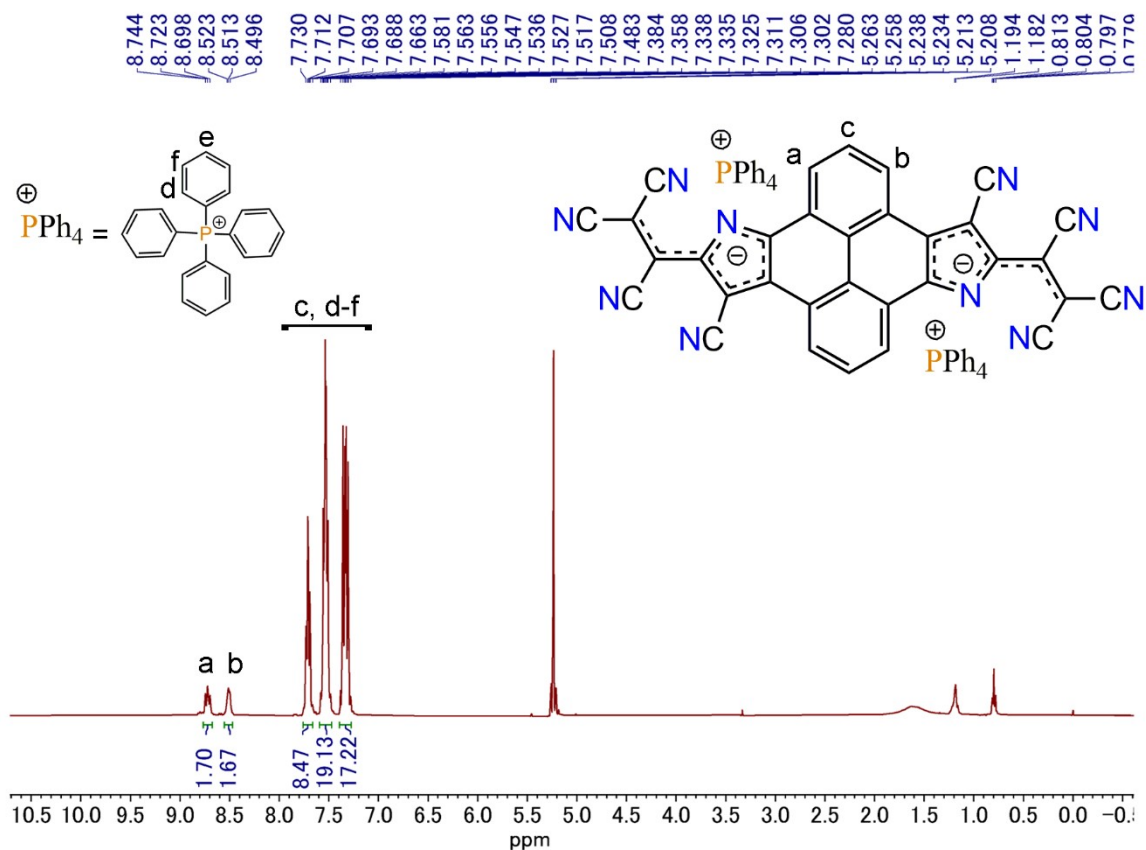


Figure S20: 400 MHz ^1H NMR spectrum of molecule **2** at RT in CD_2Cl_2 .

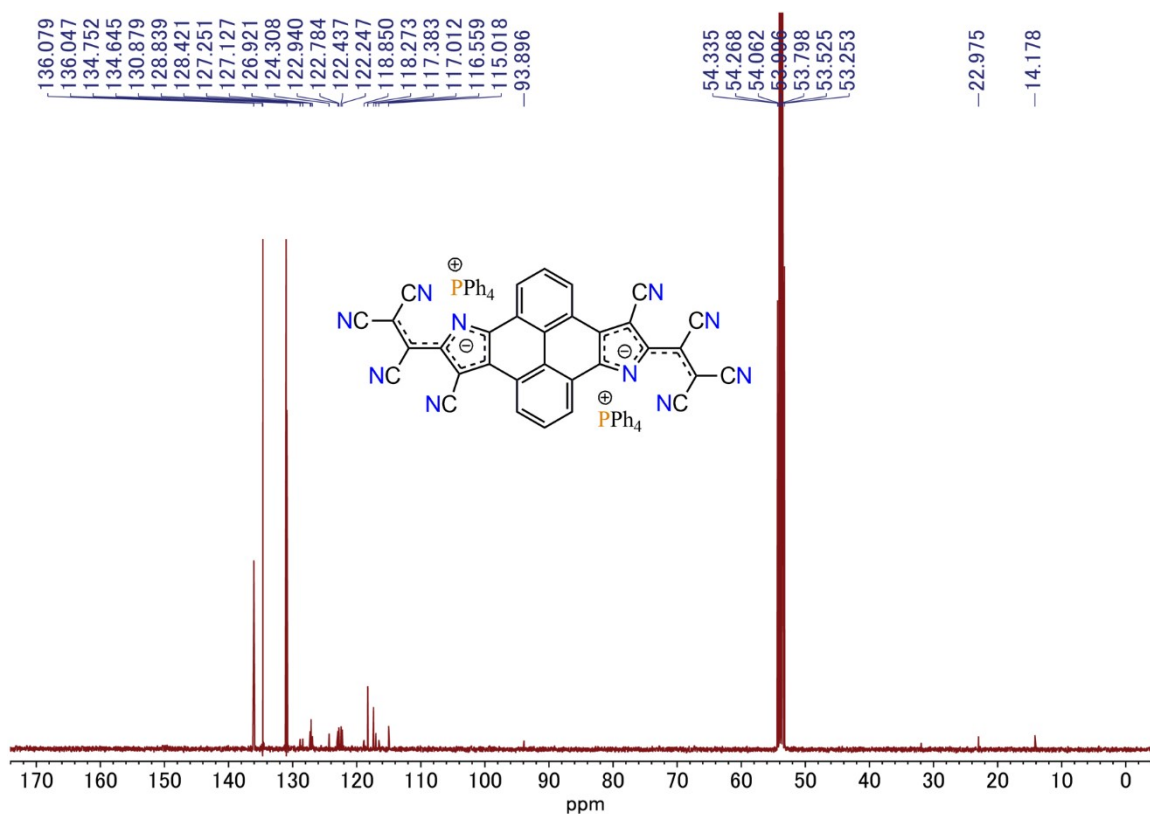


Figure S21: 100 MHz ^{13}C NMR spectra of molecule **2** at RT in CD_2Cl_2 .

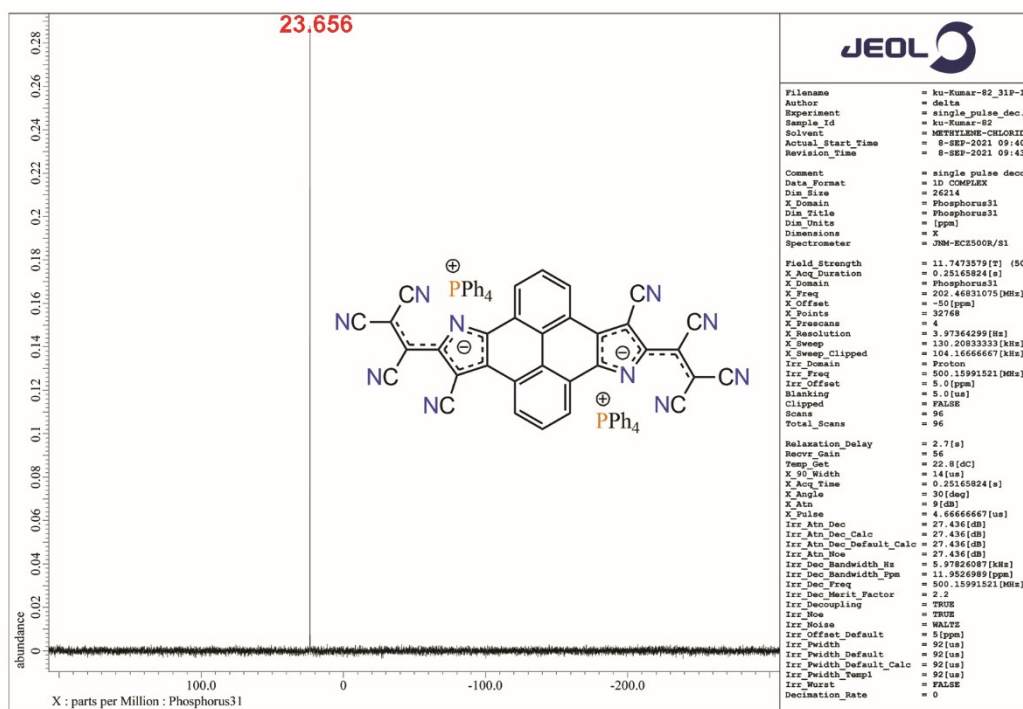


Figure S22: 202 MHz ^{31}P NMR spectrum of molecule **2** at RT in CD_2Cl_2 .

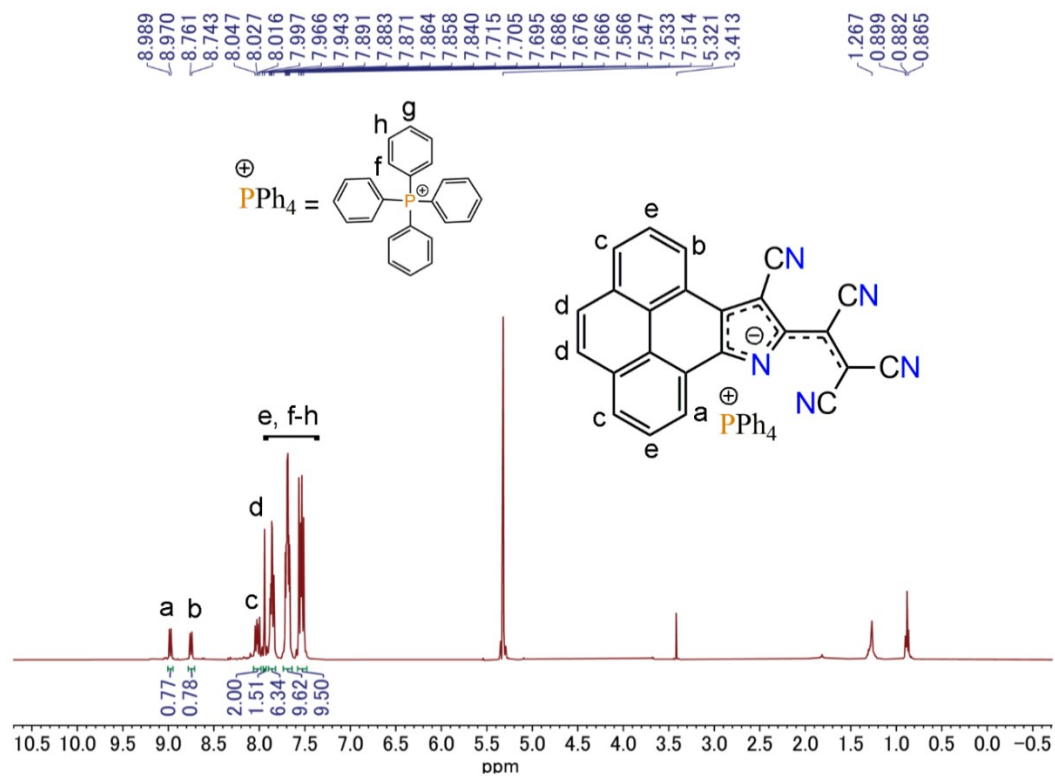


Figure S23: 400 MHz ^1H NMR spectrum of molecule **3** at RT in CD_2Cl_2 .

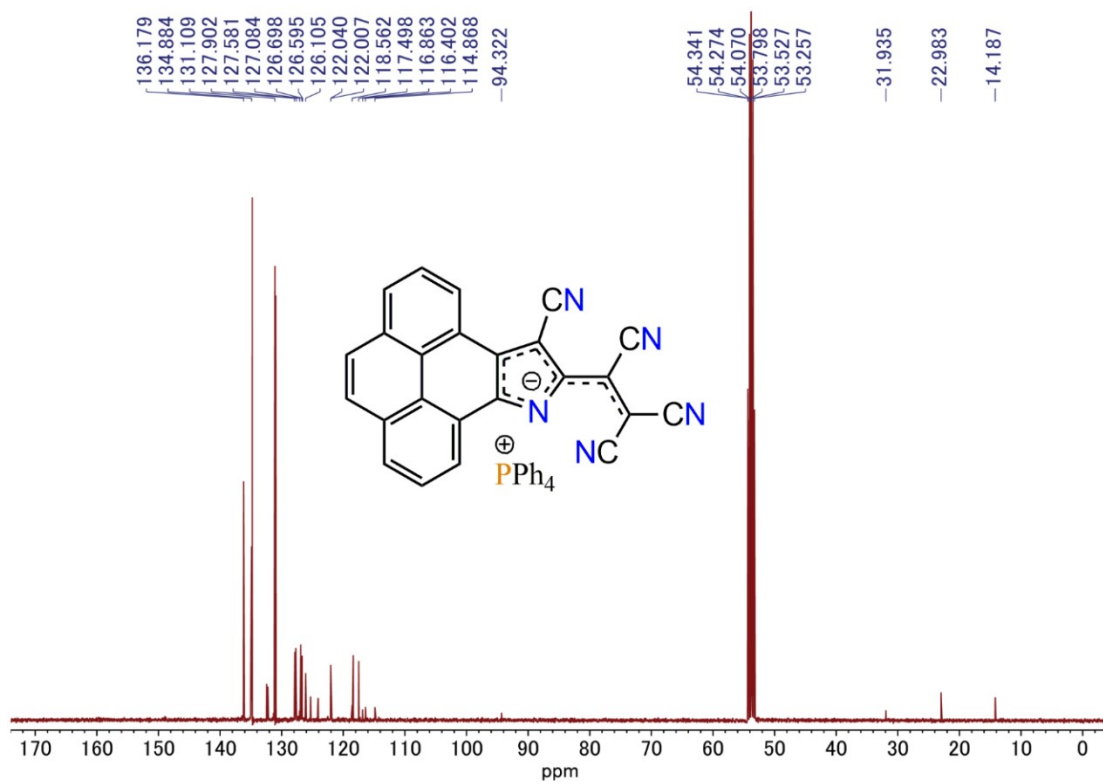


Figure S24: 100 MHz ^{13}C NMR spectra of molecule **3** at RT in CD_2Cl_2 .

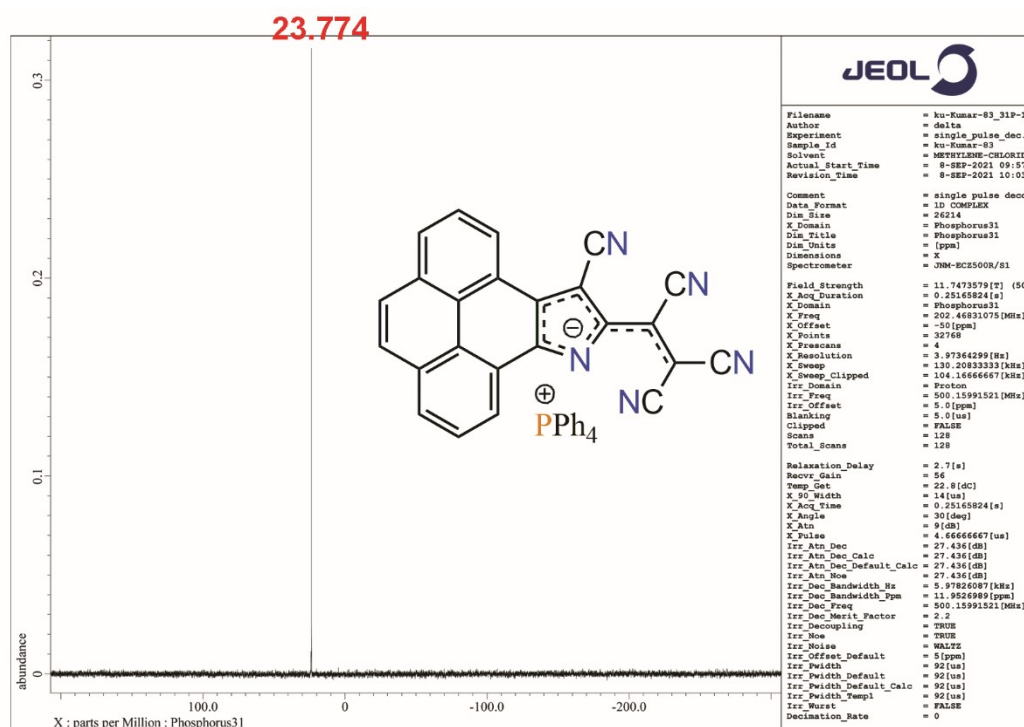


Figure S25: 202 MHz ^{13}P NMR spectrum of molecule **1** at RT in CD_2Cl_2 .

References:

1. A. D. Becke, *J. Chem. Phys.*, **1993**, *98*, 5648.
2. C. Lee, W. Yang and R. G. Parr, *Phys. Rev. B*, **1988**, *37*, 785.
3. Gaussian 16, Revision C.01, M. J. Frisch, G. W. Trucks, H. B. Schlegel, G. E. Scuseria, M. A. Robb, J. R. Cheeseman, G. Scalmani, V. Barone, G. A. Petersson, H. Nakatsuji, X. Li, M. Caricato, A. V. Marenich, J. Bloino, B. G. Janesko, R. Gomperts, B. Mennucci, H. P. Hratchian, J. V. Ortiz, A. F. Izmaylov, J. L. Sonnenberg, D. Williams-Young, F. Ding, F. Lipparini, F. Egidi, J. Goings, B. Peng, A. Petrone, T. Henderson, D. Ranasinghe, V. G. Zakrzewski, J. Gao, N. Rega, G. Zheng, W. Liang, M. Hada, M. Ehara, K. Toyota, R. Fukuda, J. Hasegawa, M. Ishida, T. Nakajima, Y. Honda, O. Kitao, H. Nakai, T. Vreven, K. Throssell, J. A. Montgomery, Jr., J. E. Peralta, F. Ogliaro, M. J. Bearpark, J. J. Heyd, E. N. Brothers, K. N. Kudin, V. N. Staroverov, T. A. Keith, R. Kobayashi, J. Normand, K. Raghavachari, A. P. Rendell, J. C. Burant, S. S. Iyengar, J. Tomasi, M. Cossi, J. M. Millam, M. Klene, C. Adamo, R. Cammi, J. W. Ochterski, R. L. Martin, K. Morokuma, O. Farkas, J. B. Foresman, and D. J. Fox, *Gaussian, Inc., Wallingford CT*, **2019**.
4. J. Hu, D. Zhang, F. W. Harris, *J. Org. Chem.* **2005**, *70*, 707-708.